

Vibrationally-resolved X-ray spectra of diatomic systems. I. Time-independent simulations with density functional theory

Lu Zhang¹, Minrui Wei¹, Guoyan Ge¹, and Weijie Hua^{*,1}

¹MIIT Key Laboratory of Semiconductor Microstructure and Quantum Sensing, Department of Applied Physics, School of Science, Nanjing University of Science and Technology, 210094 Nanjing, China

* E-mail: wjhua@njjust.edu.cn (W. Hua)

July 27, 2023

Abstract

We performed a systematic first-principles study on vibrationally-resolved X-ray absorption (XAS) and photoelectron (XPS) spectra of a series of diatomic molecules and cations (XAS, N_2 , N_2^+ , NO^+ , CO , CO^+ ; XPS, CO) at the C/N/O K-edges. All computations were done in a time-independent (TI) framework under the harmonic oscillator approximation. To evaluate the performance of different functionals, two common pure (BLYP and BP86) and two hybrid (B3LYP and M06-2X) functionals were used. Excellent agreement between theoretical and experimental spectra was observed in most systems. Two instances, where the peak separations were underestimated, were seen in the O1s XAS spectra of CO and NO^+ , and we explain this discrepancy to the anharmonic effects. The functional dependence can be evident or negligible, depending on the specific system and spectrum under consideration. In all these examples, the pure functionals exhibit a better or similar spectral accuracy to the hybrid functionals. This was attributed to better accuracy in bond lengths and vibrational frequencies (in both the initial and final states) predicted by pure functionals, as compared with the experiments. Structural and frequency changes induced by the core hole were summarized. We highlight the use of density functional theory with pure functionals for such diatomic calculations for easy execution and generally reliable accuracy.

1 Introduction

Spectroscopy links experiment and theory, with precision at the heart. An illustrative example in the history of physics is the hydrogen spectrum, where esca-

lating measurement precision has reciprocally fostered the evolution of quantum theory. High-resolution spectroscopy acts as a litmus test for gauging the precision of theoretical methods used. Particularly, in the context of high-resolution vibrationally-resolved X-ray spectroscopy,[1, 2, 3, 4, 5, 6, 7, 8, 9, 10, 11, 12, 13, 14, 15] comparison to experimental data affords an evaluation of the quality of potential energy surfaces (PESs) for both the core-electron excited (or ionized) and the ground electronic states. It also provides opportunities to scrutinize the accuracy of employed electronic structure methods, especially when dealing with states that encompass a core hole.

Density functional theory (DFT) has emerged as a predominant electronic structure method, offering profound insights into a broad spectrum of molecules and materials. It holds the capability to accurately predict X-ray spectra.[16] The conjunction of DFT with the Duschinsky rotation (DR) method[17] has yielded substantial alignment with experiments for vibrationally-resolved X-ray photoelectron (XPS)[18, 19, 20] and absorption (XAS)[21] spectra, spanning a comprehensive spectrum of molecules, such as benzene,[18] furan,[18] pyridine,[18] azines,[19] polycyclic aromatic hydrocarbons (PAHs),[20] and ions like N_2H^+ .[21] In these calculations, either full core-hole (FCH) or excited core-hole (XCH)[22] approximation was leveraged to describe the core ionized (in the case of XAS) or excited (in the case of XPS) states, while conventional DFT was employed to model the ground state (GS). (In the subsequent context, the term “excited state” is used without distinction to refer to either a core excited or ionized state.) It is worth noting of other DFT applications[8, 23, 18] also with the half core hole (HCH)[24] or the equivalent core hole (ECH, i.e., $Z+1$)[25] approximations. Buoyed by the promising outcomes from DFT computations, we are currently engaged in formulating a theoretical library for vibrationally-resolved XPS/XAS spectra of common molecules and ions, with initial findings already disseminated.[18, 19, 20] Most investigated systems were polyatomic, i.e., composed of three or more atoms.

A diatomic system, with a single vibrational mode, offers a more “transparent” view of vibronic coupling effects and is highly sensitive to the utilized electronic structure method. Diatomic molecules such as N_2 ,[26] CO ,[27] NO ,[27] and ions like NH^+ ,[28] N_2^+ ,[29] CO^+ ,[30] NO^+ ,[31] and C_2^- [15] have been extensively investigated through both XPS/XAS experiments[26, 27, 2, 28, 29, 30, 31, 15] and simulations at varied levels.[1, 26, 27, 28, 29, 30, 31, 15] Generally, the results indicate good agreement. Alongside technological advancements in X-ray synchrotron beams for experimental development[10], theoretical methods for X-ray spectra have also seen significant improvements in recent years[1], enabling high-quality theoretical predictions of vibrationally resolved X-ray spectra. Neutral diatomic molecules have been a frequent focus in many X-ray spectral studies due to their ability to reach higher target densities compared to charged particles[15]. Recent innovations in ion beam and ion trap techniques have facilitated precise inner-shell investigations involving positively charged diatomic molecular ions.[31, 28]

We found that various post-Hartree-Fock methods were used in almost all calculations. Couto et al.[30] presented and analyzed high-resolution XAS spec-

tra of CO^+ , using wavepacket dynamics calculations based on potential energy curves (PECs) computed with the restricted active space second-order perturbation (RASPT2) method. Using the restricted active space multiconfigurational theory self-consistent field (RASSCF) and second-order perturbation (RASPT2) methods, Lindblad et al. interpreted the experimental XAS spectra of N_2^+ [29] and NO^+ . [31] Carniato et al. [28] simulated the PECs of low-lying $\text{N}1s$ excited states of NH^+ by using the configuration interaction singles and doubles (CISD) method and the valence-state PECs by multiconfigurational self-consistent field (MCSCF). Rocha [32] simulated PEC of CO in the lowest $\text{C}1s$ excited state by the restricted active space SCF (RASSCF) method, termed also as the inner-shell complete active space SCF (IS-CASSCF) method. Martins et al. [33] computed PECs of low-lying $\text{F}1s$ core excited states of HF and HF^+ by using the full configuration-interaction method to help understand the photodissociation dynamics. Such studies have been instrumental in enriching our understanding of core-hole state electronic structure, X-ray physics, vibronic coupling, and bond dissociation dynamics. However, such studies typically cover one or only a few systems. Computational studies by different groups frequently take different theoretical levels. There is a lack of simulations of many systems on the same footing, which is essential for enabling fair comparisons and analyses to draw general rules concerning vibronic coupling properties.

The aim of this study is to benchmark the application of DFT in simulating vibrationally-resolved XPS/XAS spectra of diatomic systems. This premise is built upon the ability of DFT to generate accurate potential energy curves (PECs) in close proximity to the Franck-Condon region, despite its potential shortcomings at larger bond distances where multi-configurational effects become pivotal. In this work, the FCH approximation will be deployed for the $1s$ ionized state and the XCH approximation for the lowest $1s$ excited state. A variety of common molecules and ions will be used for the XAS (N_2 , N_2^+ , NO^+ , CO , and CO^+) and XPS (CO) spectra, covering the C/N/O K-edges.

Generally, two complementary solutions to vibronic coupling include the time-independent (TI) and time-dependent (TD) frameworks. The TI method is usually based on the harmonic oscillator approximation and mathematically represented by an analytical sum-over-states expression. [34] It involves optimizing the structure of the final state and performing vibrational frequency calculations, which can be challenging for certain systems. [19, 35] However, the spectral interpretations obtained through the TI approach are direct and straightforward. On the other hand, the TD wavepacket method is based on the Fourier transform of the auto-correlation function. [36, 30] This method allows for the inclusion of anharmonic effects that can be included from the input potential energy surfaces. In this study, we specifically present the results obtained using the TI framework. We plan to utilize the TD method in a subsequent study (paper II) [37] in order to get a complete picture.

2 Time-independent method

We use bolded symbols in lower and upper cases for vectors and matrices, respectively, while symbols in normal fonts indicate scalars. The initial (ground) electronic state is denoted by g , and the final (core-excited or core-ionized) electronic state by e . We differentiate any physical quantity in state g or e using a respective symbol with or without a prime. As such, equilibrium geometries (expressed as Cartesian coordinates in column vectors) of the initial and final states are denoted by \mathbf{x}' and \mathbf{x} ; normal coordinates (also in column vectors) for both states are represented by \mathbf{q}' and \mathbf{q} ; respective normal mode matrices are signified by \mathbf{L}' and \mathbf{L} ; vibrational frequencies are designated by ω' and ω ; and bond lengths are represented by R' and R .

The time-independent method was considered based on the harmonic oscillator approximation. Vibrational frequency calculations were first performed at the optimized geometries of both the initial and the final electronic states. The Duschinsky rotation (DR) method[17] was then used to connect both normal coordinates:

$$\mathbf{q}' = \mathbf{J}\mathbf{q} + \mathbf{k}. \quad (1)$$

Here \mathbf{k} indicates the displacement vector between the PESs of both electronic states along the normal coordinate. \mathbf{J} is the Duschinsky rotation matrix, which is 1 for a diatomic system. \mathbf{k} depends on the initial-state normal coordinate matrix \mathbf{L}' , the diagonal matrix of atomic masses \mathbf{M} , and the change between the equilibrium geometries of both states $\Delta\mathbf{x}$ ($\Delta\mathbf{x} \equiv \mathbf{x} - \mathbf{x}'$):

$$\mathbf{k} = (\mathbf{L}')^T \mathbf{M}^{1/2} \Delta\mathbf{x}. \quad (2)$$

The vibrational profile can then be calculated with \mathbf{k} and the vibrational frequencies (ω' and ω).[38, 39, 40]

The 0-0 vibrational transition energy in XAS and XPS spectra are respectively calculated by using the Δ Kohn-Sham (Δ KS) scheme,[41, 42]

$$E_{00}^{\text{XAS}} = E_{\text{XCH}}|_{\min \text{XCH}} - E_{\text{GS}}|_{\min \text{GS}} + \delta_{\text{rel}}, \quad (3)$$

$$E_{00}^{\text{XPS}} = E_{\text{FCH}}|_{\min \text{FCH}} - E_{\text{GS}}|_{\min \text{GS}} + \delta_{\text{rel}}, \quad (4)$$

which considers both electronic and geometrical relaxations. Here E_{GS} , E_{FCH} , and E_{XCH} stand for total energies of the ground electronic state, the FCH state with one 1s electron removed, and the XCH state with one 1s electron excited to the lowest unoccupied molecular orbital (LUMO), respectively; **min GS**, **min FCH**, or **min XCH** denotes the optimized structure of each state. δ_{rel} is a small uniform shift considering the differential relativistic effect, which is related to the removal of an electron from the core orbital. The values used for the C, N, and O 1s core holes are $\delta_{\text{rel}} = 0.2, 0.3,$ and 0.4 eV, respectively.[42]

3 Computational details

All time-independent calculations were carried out at the DFT level by using the GAMESS-US package.[43, 44] Four different functionals were chosen:

BLYP,[45, 46] BP86,[45, 47] B3LYP,[48, 46] and M06-2X.[49] The aug-cc-pVTZ basis set[50, 51] was used in the optimization of the ground state. In the excited state, the IGLO-III basis set[52] was set for the excited atom. For systems that include two atoms of the same element (N_2 and N_2^+), model core potential (MCP) together with corresponding MCP/TZP basis set[53, 54, 55] was employed for the non-excited atom.

All simulations were performed by enforcing the C_{4v} point group symmetry. Cartesian coordinates of all optimized geometries are provided in the Supplementary Material.[56]

After performing geometrical optimizations and vibrational frequency calculations for both the ground and excited states, a modified DynaVib package [18] was employed to compute the Franck-Condon factors (FCFs). The vibrationally-resolved XAS and XPS spectra were obtained by convoluting the stick FCFs with a Lorentzian function. A hwhm value, $\gamma=0.05$ eV, was chosen to achieve better agreement with experimental observations. Here γ is to phenomenologically include many effects for broadening (such as the lifetime and instrumental broadening, environmental effects) and similar values have been utilized in previous studies for other systems.[18, 19, 35, 20] In practice, one may use the Voigt convolution (see, e.g., Ref. [21]) to tune a better agreement with the experiment, with the Lorentzian/Gaussian hwhm values read a library,[57] or directly from the experiment.[21] However, in this work, the hwhm parameter is not considered as a pivotal factor. For simplicity and consistency, a constant hwhm value was utilized in all calculations, which does not impact the validity of our discussions.

4 Results and discussion

4.1 Bond lengths and core-hole induced changes

Table 1 shows the bond lengths in both the ground (R') and excited (R) states of 10 examples located by four different functionals, as well as their differences, $\Delta R \equiv R - R'$. To more vividly show the comparisons with the gas phase experiments, this information is visualized in Fig. 1. The experimental bond lengths in the gas phase show a narrow region of $R' = 1.063\text{--}1.128$ Å, spanning over 0.065 Å. The 1s core excitation/ionization can either increase (by 0.025–0.163 Å) or decrease (by 0.037–0.065 Å) the bond lengths, depending on the system and the excited atom. This corresponds to positive or negative ΔR [see also Fig. 1(b)]. In the excited state, the bond lengths span a much wider range of 0.228 Å ($R = 1.063\text{--}1.291$ Å).

In general, our theoretical results by all functionals match well with the experiments [Table 1; Fig. 1(a)]. The mean absolute deviations (MADs) predicted by BLYP, BP86, B3LYP, and M06-2X functionals for R (R') are 0.008, 0.006, 0.008, 0.014 (0.008, 0.008, 0.005, 0.010) Å, respectively. The maximum absolute deviations (MAXs) are 0.017, 0.017, 0.027, 0.037 (0.010, 0.010, 0.011, 0.017) Å. The relative errors for R (R') are 0.2%–1.6%, 0.0%–1.6%, 0.1%–2.3%,

0.2%–3.4% (0.0%–0.9%, 0.1%–0.9%, 0.2%–1.0%, 0.5%–1.5%). Correspondingly for ΔR , the deviations are 0.001–0.008, 0.000–0.007, 0.001–0.020, 0.001–0.022 Å.

The deviations from the experiments look almost invisible for R or R' [Fig. 1(a)] and small for ΔR [Fig. 1(b)]. Our results show that the pure functionals BLYP and BP86 (very close) generally provide an even better agreement with the experiments than the two hybrid functionals B3LYP and M06-2X. Specifically, with the two pure functionals, the best agreement with the experiments locates in N_2^+ , with absolute deviations of only 0.000–0.002 Å to the corresponding experiment.[29] The second best is N_2 , with absolute deviations of only 0.000–0.005 Å to the experiments.[58] The corresponding changes in bond length ΔR for N_2^+ and N_2 are 0.038–0.038 and 0.061–0.063 Å, respectively. Meanwhile, B3LYP and M06-2X predict the worst agreement in ΔR for N_2^+ and N_2 among all examples [Fig. 1(b)]: the deviations by B3LYP are 0.014 and 0.020 Å, and those by M06-2X are 0.021 and 0.022 Å.

4.2 Vibrational frequencies and core-hole induced changes

Table 2 lists the vibrational frequencies in both the initial (ω') and final (ω) states with comparisons to experiments. The experimental vibrational frequencies cover a range of 2169.8–2376.7 cm^{-1} (206.9 cm^{-1}) in the ground state geometry and a much wider range of 1338.9–2507.6 cm^{-1} (1168.7 cm^{-1}) in the excited state one. The values are typical frequencies for stretching vibrational modes. Similarly to the bond lengths, the influence of the core hole has no definite change directions, that is, both frequency increase and decrease are found.

The deviations of our DFT calculations to experiments seem to be larger than the bond lengths. This is because the vibrational frequency corresponds to the second-order energy derivatives of the Cartesian coordinates. BLYP, BP86, B3LYP, and M06-2X had MAD values of 38.5, 33.8, 111.7, 200.7 (44.2, 34.5, 73.3, 156.0) cm^{-1} for ω (ω'), and MAX values are 74.1, 73.0, 315.0, 475.4 (55.3, 48.8, 122.8, 210.9) cm^{-1} . The relative deviations for ω (ω') are 0.9%–5.5%, 0.1%–3.7%, 0.4%–13.0%, 2.3%–20.0% (1.0%–2.6%, 0.6%–2.3%, 1.9%–5.6%, 4.8%–9.1%). Additionally, Table 2 also shows the vibrational frequency change in the initial and final states, $\Delta\omega \equiv \omega - \omega'$. Correspondingly, the deviations are 3.5–82.0, 2.0–96.2, 11.4–192.2, 12.5–275.7 cm^{-1} .

The deviations for ω' or ω are small for the pure functionals and acceptable for the hybrid functionals [Fig. 1(c)]. Concerning $\Delta\omega$, the deviations by BLYP or BP86 are small, while the results by B3LYP or M06-2X are acceptable for most examples [Fig. 1(d)]. Specifically, the largest deviation happens in N_2^+ , which is 192.2 cm^{-1} by B3LYP and 275.7 cm^{-1} by M06-2X, respectively.

The analysis of vibrational frequencies supports the same conclusion as the bond lengths that pure functionals produce better results than hybrid functionals. Our accuracy in vibrational frequencies is reasonable considering the absolute values of experimental frequencies are some 2100–2400 cm^{-1} in the ground state and 1300–2500 cm^{-1} in the excited state. Besides, our DFT calcu-

lations predicted balanced accuracy in both the ground and excited states, since the MADs (of the same functional) are close. Similar accuracy was obtained in other calculations. For instance, Moitra et al.[59] achieved an overestimation of 90 cm^{-1} ($2233\text{ versus }2143\text{ cm}^{-1}$) and 102 cm^{-1} ($2432\text{ versus }2330\text{ cm}^{-1}$) for CO and N_2 , respectively, in the ground state by using the MP2 method.

4.3 XAS of N_2 and N_2^+

Figures 2-5 display the simulated vibrationally-resolved XAS spectra of N_2 , N_2^+ , NO^+ , CO, and CO^+ , respectively, computed by DFT with four different functionals. For each molecule, the spectra computed by the four functionals show evident differences. That is, the fine structures are sensitive to the choice of functionals for these diatomic systems. It is worth noting that weak functional dependence was observed in the vibrationally-resolved N1s XPS spectrum of pyrimidine ($\text{C}_4\text{H}_4\text{N}_2$).[19] It appears that the functional sensitivity is washed away by multiple vibrational modes. In most case studies, theoretical results agree well with corresponding experiments.

Figure 2 displays our computed N1s XAS of N_2 and N_2^+ in comparison with the experiments.[6, 60, 29] In Fig. 2(a), the experimental spectrum has 5 clear vibronic features, where the 0-0 and 0-1 peaks have almost equal intensities. Our BLYP and BP86 calculations predicted both accurate peak separations (i.e., to the vibrational frequencies) and relative peak intensities. As we know, in a diatomic system, the peak separation is equivalent to the vibrational frequency, and the agreement in separation here is consistent with the discussion above in Section 4.2 (see also Table 2). BLYP gives almost identical intensities of the 0-0 and 0-1 peaks, exhibiting the best agreement with the experiment. BP86 shows a slightly weaker 0-1 peak than the 0-0 peak. B3LYP and M06-2X predicted relatively large peak separations. The predicted 0-1 peak intensity is about 2/3 of the 0-0 peak. Our results show a better performance of the pure than hybrid functionals.

In Fig. 2(b), the 0-0 experiment peak of N_2^+ (394.29 eV) exhibits a red-shift of 7.20 eV compared with N_2 (401.49 eV), in line with the valence shell ionization. Besides, in the experimental spectrum, three vibronic features are evident, with the 0-1 peak having almost half the intensity compared to the 0-0 peak. Similarly, BLYP and BP86 predicted peak separations in good agreement with the experiment, and they reproduced the relative peak intensities with a slight underestimation of the 0-1 peak intensities. B3LYP and M06-2X slightly overestimated the peak separations. They also overestimated the 0-1 peak intensity compared with the 0-0 one, showing a slower decay in intensity than the experiment with respect to the increasing vibrational quantum number n .

4.4 XAS of NO^+

Figure 3 displays the XAS results of NO^+ in both the N1s and O1s edges. In the N1s edge (panel a), all functionals show good agreement with the experiment.[31] The experiment spectrum distinguished five vibronic features with the 0-0 and

0-1 peaks having almost equal intensities. The pure functionals predicted good agreement in peak separations, while they slightly underestimate the 0-1 intensities and show a quicker decay with n . Meanwhile, B3LYP and M06-2X slightly overestimated the peak separations, and the peak intensities agree well with the experiment (almost equal 0-0 and 0-1 intensities).

In the O1s edge (panel b), the experiment spectrum[31] shows more complex structures with 10 relatively weak vibronic features. To some extent, it also seems difficult to unambiguously distinguish the 0-0 peak. All four functionals predicted similar theoretical spectra. They give only acceptable agreement with the experiment: the general peak profile shapes are similar but the theory underestimated the peak separations.

This seems to be a difficult case for theoretical simulations. We think the major reason cannot be assigned to the electronic structure method used as the performance of different functionals is similar. We ascribe the reason to the harmonic oscillator approximation used. This is consistent with the fact that O1s core excitation in NO^+ induced a large change in the potential energy surface, both in the equilibrium position and the curvature. The bond length was changed by $+0.140 \text{ \AA}$ (from 1.063 to 1.203 \AA) and the vibrational frequency was changed by -841.8 cm^{-1} (from 2376.7 to 1534.9 cm^{-1}). They correspond respectively to the second largest (Table 1) and the largest (Table 2) changes among all examples. More accurate calculations are expected by considering anharmonic effects.

4.5 XAS of CO and CO^+

CO and NO^+ are isoelectronic species. The results of CO show very similar performance to NO^+ . As shown in Fig. 4, in the C1s edge, the experimental spectrum resolved only two simple features while in the O1s edge, it generates about 12 weak features in a broad peak. All functionals generated spectra with less functional dependence. They all predict good agreement to the experiment in the C1s edge and acceptable agreement in the O1s edge. All theories underestimate the peak separations in the O1s edge, similar to the case of NO^+ in the O1s edge. The underlying structural reason is also the drastic changes in the PEC as induced by the O1s core excitation. The change in bond length is $+0.163 \text{ \AA}$ (from 1.128 to 1.291 \AA) and that in vibrational frequency is -830.9 cm^{-1} (from 2169.8 to 1338.9 cm^{-1}), which are the largest (Table 1) and the second largest (Table 2) among all examples.

The case of CO^+ is much simpler. Figure 5 displays the XAS spectra of CO^+ in both the C1s and O1s edges. The valence-shell ionization (from CO to CO^+) leads to a red shift of the experimental 0-0 peak in both edges: -5.25 eV (from 287.29 to 282.04 eV) in the C1s edge and -5.20 eV (from 533.62 to 528.42 eV) in the O1s edge. In both edges, the experimental spectra[30] resolved three vibronic fine structures. All functionals produce a good agreement with the experiments both in energies and profiles, showing only weak functional dependence.

4.6 XPS of CO

All examples above are on XAS spectra. Figure 6 displays the simulated vibrationally-resolved XPS spectra of CO at the C and O 1s edges. In comparison to the XAS experiments, the 0-0 peak in both edges exhibits blue shifts: +8.84 eV (from 287.29 to 296.13 eV) and +9.00 eV (from 533.62 to 542.62 eV), respectively. The experimental XPS spectra[2] show simple vibronic features at both edges, and all theory well reproduced the experimental spectra. Specifically, the hybrid functional M06-2X seems to slightly overestimate the 0-1 peak intensity in the C1s edge [Fig. 6(a)]. By comparing the XAS [Fig. 4(b)] and XPS [Fig. 6(b)] spectra of CO at the O1s edge, one can find the different responses of the final-state PES induced by O1s excitation and ionization. This may be related to the odd or even number of electrons.

5 Summary and Conclusions

To summarize, in the time-independent framework with the harmonic oscillator approximation, we have systematically assessed the vibrationally-resolved XAS (N_2 , N_2^+ , NO^+ , CO , CO^+) and XPS (CO) spectra of a series of diatomic systems by DFT with four different functionals. In most cases, the theoretical X-ray spectra match well with the experiments both in absolute energies and profiles. For two exceptions (O1s XAS of NO^+ and CO), theory predicted similar but shrunk profiles (i.e., the peak separations were underestimated) which were attributed to the strong anharmonic effects. With geometries of the 1s excited/ionized states located, bond lengths and vibrational frequencies were compared with the initial states to see the core hole effects. Comparisons with experiments show good agreement, and the pure functionals (BLYP and BP86) generally predicted better or similar agreement than the two hybrid functionals (B3LYP and M06-2X). The sensitivity of different functional depends on systems: evident dependence was observed in XAS spectra of N_2 , N_2^+ , and NO^+ , while weak dependence was also found in the rest cases. Our study provides a systematic assessment of the DFT method in simulating vibrationally-resolved XAS/XPS spectra in the TI framework with the harmonic oscillator approximation. We shall analyze in detail the anharmonic effects in the time-dependent framework in a subsequent study.[37]

Acknowledgments

Financial support from the National Natural Science Foundation of China (Grant No. 12274229) and the Postgraduate Research & Practice Innovation Program of Jiangsu Province (Grant Nos. KYCX22_0425 and KYCX22_0424) is greatly acknowledged.

Table 1: Comparison of bond lengths (in Å) in the optimized ground (R') and 1s excited/ionized (R) states of selected diatomic systems by the DFT method with different functionals.

Compound	Expt.			BLYP			BP86			B3LYP			M06-2X		
	R'	R	ΔR^a	R'	R	ΔR	R'	R	ΔR	R'	R	ΔR	R'	R	ΔR
N ₂	1.098 ^{e, f}	1.164 ^{f, i}	+0.066	1.103	1.167	+0.063	1.103	1.164	+0.061	1.092	1.137	+0.046	1.087	1.130	+0.044
N ₂ ⁺	1.116 ^f	1.076	-0.040 ^j	1.116	1.078	-0.038	1.115	1.078	-0.038	1.105	1.051	-0.054	1.099	1.039	-0.061
NO ⁺ (N) ^b	1.063 ^g	1.123	+0.060 ^k	1.072	1.129	+0.058	1.071	1.125	+0.055	1.057	1.117	+0.059	1.050	1.109	+0.059
NO ⁺ (O)	1.063	1.203	+0.140 ^k	1.072	1.211	+0.139	1.071	1.205	+0.134	1.057	1.199	+0.141	1.050	1.193	+0.142
CO(C)	1.128 ^{f, h}	1.153 ^f	+0.025	1.138	1.164	+0.026	1.138	1.161	+0.023	1.126	1.156	+0.029	1.122	1.155	+0.034
CO(O)	1.128	1.291 ^h	+0.163	1.138	1.300	+0.162	1.138	1.295	+0.157	1.126	1.292	+0.165	1.122	1.293	+0.172
CO ⁺ (C)	1.115 ^f	1.078	-0.037 ^l	1.125	1.080	-0.045	1.124	1.080	-0.044	1.110	1.068	-0.043	1.102	1.059	-0.044
CO ⁺ (O)	1.115	1.162	+0.047 ^l	1.125	1.176	+0.051	1.124	1.175	+0.051	1.110	1.163	+0.052	1.102	1.156	+0.054
CO(C)[XPS] ^c	1.128	1.063	-0.065 ^m	1.138	1.080	-0.058	1.138	1.080	-0.059	1.126	1.068	-0.059	1.122	1.059	-0.063
CO(O)[XPS]	1.128	1.165	+0.037 ^m	1.138	1.176	+0.038	1.138	1.175	+0.037	1.126	1.163	+0.036	1.122	1.156	+0.035
MAD ^d	-	-	-	0.008	0.008	0.003	0.008	0.006	0.004	0.005	0.008	0.006	0.010	0.014	0.008
MAX ^d	-	-	-	0.010	0.017	0.008	0.010	0.017	0.007	0.011	0.027	0.020	0.017	0.037	0.022

^a $\Delta R \equiv R - R'$, changes of bond length in Å.

^b For compound with two different elements, the core excitation/ionization center is specified in parenthesis.

^c [XPS] denotes comparison of initial and final states involved in XPS. The rest are for XAS.

^d MAD, mean absolute derivation; MAX, maximum absolute deviation.

^e Ehara et al.[26]

^f Neeb et al.[58]

^g Albritton et al.[61]

^h Püttner et al.[27]

ⁱ Chen et al.[6]

^j Lindblad et al.[29]

^k Lindblad et al.[31]

^l Couto et al.[30]

^m Hergenhahn.[2]

Table 2: Comparison of vibrational frequencies (in cm^{-1}) in the optimized ground (ω') and 1s excited/ionized (ω) states of selected diatomic systems by the DFT method with different functionals.

Compound	Expt.			BLYP			BP86			B3LYP			M06-2X		
	ω'	ω	$\Delta\omega^a$	ω'	ω	$\Delta\omega$	ω'	ω	$\Delta\omega$	ω'	ω	$\Delta\omega$	ω'	ω	$\Delta\omega$
N_2	2359.0 ^e	[†] 1966.2 [†]	-392.8	2334.9	1938.0	-396.9	2345.7	1963.5	-382.2	2449.1	2175.3	-273.8	2522.6	2255.9	-266.7
N_2^+	2207.4 ^f	[‡] 2420.8 [‡]	+213.4	2234.1	2442.3	+208.1	2253.3	2456.8	+203.5	2330.2	2735.8	+405.6	2407.2	2896.2	+489.1
$\text{NO}^+(\text{N})^b$	2376.7 ^h	1954.3 ^j	-422.4	2333.3	1987.8	-345.6	2353.6	2027.3	-326.2	2479.1	2077.5	-401.6	2587.6	2226.7	-360.9
$\text{NO}^+(\text{O})$	2376.7	1534.9 ^j	-841.8	2333.3	1512.6	-820.8	2353.6	1553.1	-800.5	2479.1	1584.1	-895.0	2587.6	1647.4	-940.2
$\text{CO}(\text{C})$	2169.8 ^f	ⁱ 2083.6 ^f	-86.2	2114.5	2015.8	-98.8	2121.0	2042.6	-78.4	2210.9	2091.3	-119.7	2273.9	2130.4	-143.5
$\text{CO}(\text{O})$	2169.8	1338.9 ⁱ	-830.9	2114.5	1264.8	-849.7	2121.0	1292.1	-828.9	2210.9	1302.0	-908.9	2273.9	1304.0	-969.9
$\text{CO}^+(\text{C})$	2214.2 ^f	2507.6 ^k	+293.4	2172.5	2478.6	+306.1	2192.0 ^m	2490.0	+298.0	2289.8	2612.5	+322.7	2393.3	2748.2	+354.9
$\text{CO}^+(\text{O})$	2214.2	1817.2 ^k	-397.0	2172.5	1779.0	-393.5	2192.0	1787.9	-404.1	2289.8	1875.3	-414.6	2393.3	1939.3	-454.0
$\text{CO}(\text{C})[\text{XPS}]^c$	2169.8	2451.9 ^l	+282.1	2114.5	2478.6	+364.1	2121.0	2490.0	+368.9	2210.9	2612.5	+401.6	2273.9	2748.2	+474.4
$\text{CO}(\text{O})[\text{XPS}]$	2169.8	1822.8 ^l	-347.0	2114.5	1779.0	-335.5	2121.0	1787.9	-333.1	2210.9	1875.3	-335.6	2273.9	1939.3	-334.5
MAD ^d	-	-	-	44.2	38.5	24.8	34.5	33.8	28.0	73.3	111.7	67.5	156.0	200.7	108.1
MAX ^d	-	-	-	55.3	74.1	82.0	48.8	73.0	96.2	122.8	315.0	192.2	210.9	475.4	275.7

^a $\Delta\omega \equiv \omega - \omega'$, changes of frequency in cm^{-1} .

^b For the compound with two different elements, the core excitation/ionization center is specified in parenthesis.

^c [XPS] denotes comparison of initial and final states involved in XPS. The rest are for XAS.

^d MAD, mean absolute derivation; MAX, maximum absolute deviation.

^e Ehara et al.[26]

^f Neeb et al.[58]

^g Laher et al.[62]

^h Albritton et al.[61]

ⁱ Püttner et al.[27]

^j Lindblad et al.[31]

^k Couto et al.[30]

^l Hergenbahn.[2]

^m By restricted open-shell DFT (RO-DFT; the rest are by unrestricted DFT).

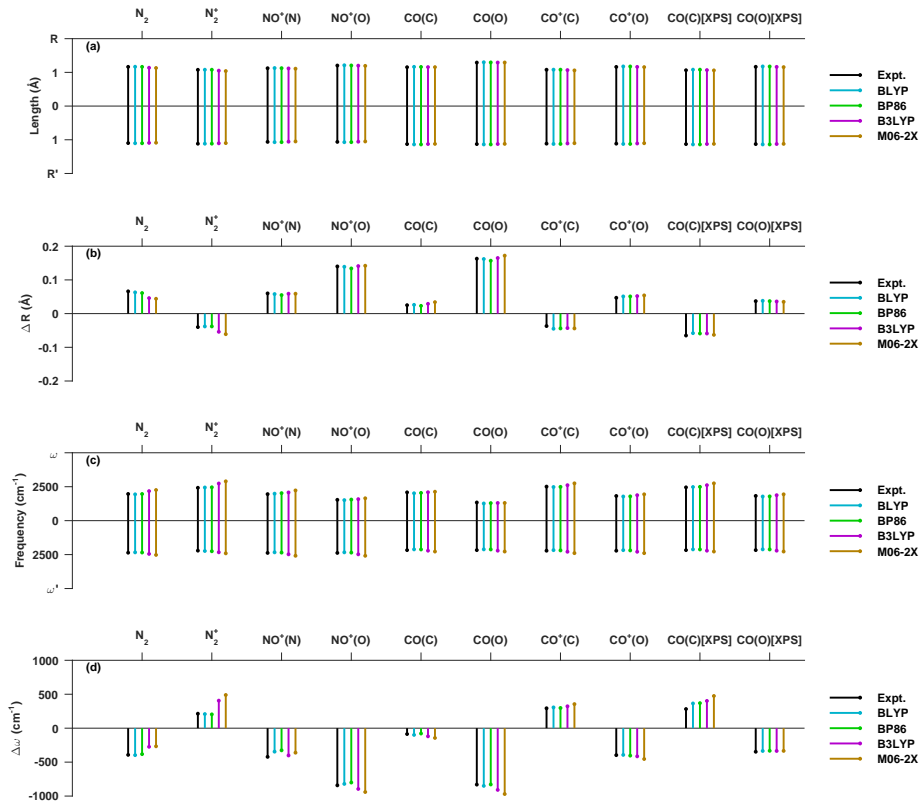


Figure 1: Comparison of parameters in the DFT-optimized structures for the ground and 1s excited/ionized states of diatomic systems with various functionals: (a) Bond lengths in the ground state (R') and excited state (R), (b) changes in bond length (ΔR), (c) vibrational frequencies in the ground state (ω') and excited state (ω), and (d) changes in frequency ($\Delta\omega$). The experimental data used for comparison are the same as those presented in Tables 1 and 2.

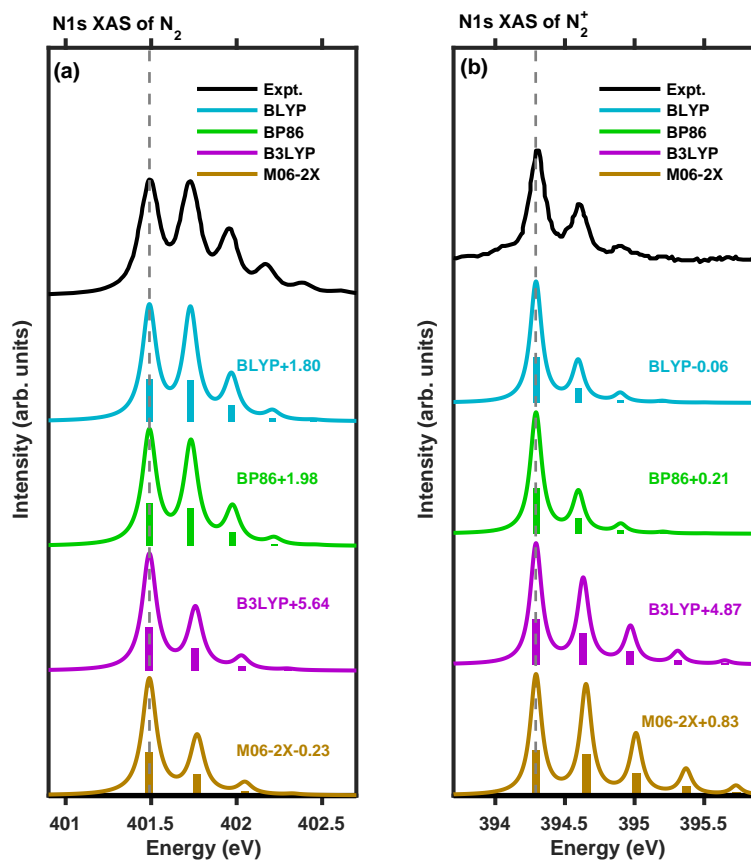


Figure 2: Vibrationally-resolved N1s XAS spectra for (a) N₂ and (b) N₂⁺ simulated with different DFT functionals in the time-independent framework. To better compare with the experiments,[6, 60, 29] theoretical spectra have been shifted (indicated by numbers in eV) by aligning the first peak.

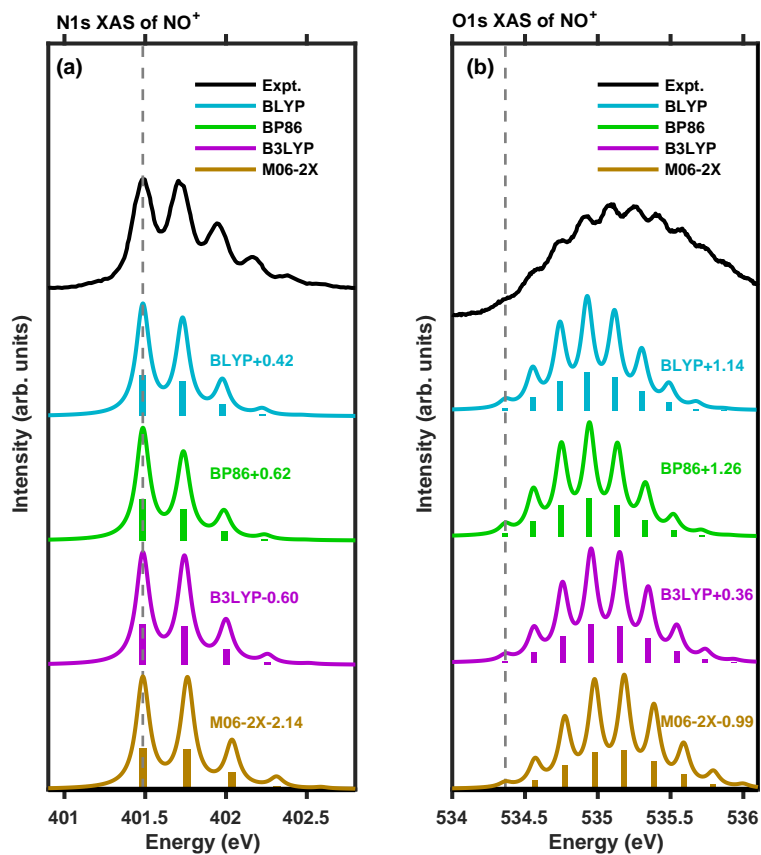


Figure 3: Vibrationally-resolved XAS spectra for NO^+ simulated with different DFT functionals in the time-independent framework: (a) N1s and (b) O1s edges. To better compare with the experiment,[31] theoretical spectra have been shifted (indicated by numbers in eV) by aligning the first peak.

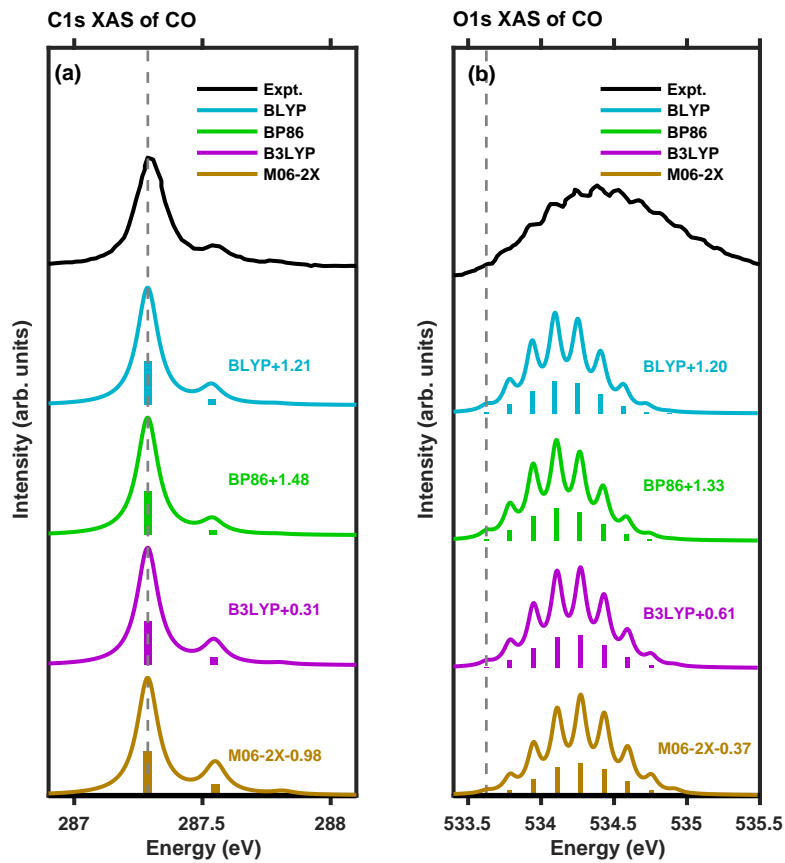


Figure 4: The same as Fig. 2 for simulated vibrationaly-resolved XAS of CO: (a) C1s and (b) O1s edges. Experiments for comparison were taken from Hitchcock et al.[60] and Püttner et al.[27]

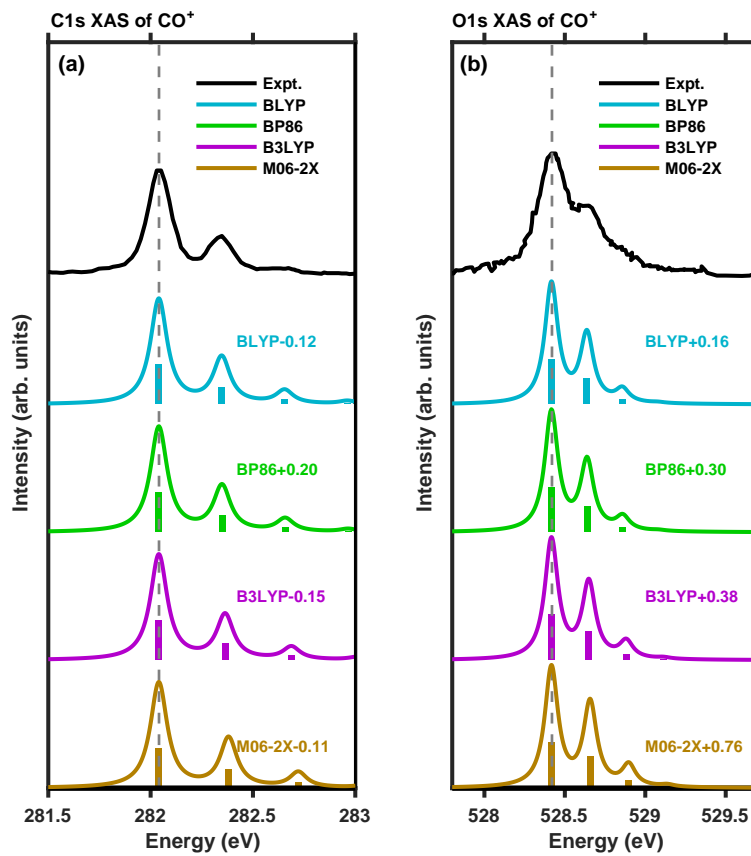


Figure 5: The same as Fig. 2 for simulated vibrationaly-resolved XAS spectra of CO^+ : (a) C1s and (b) O1s edges. Experiment was taken from Couto et al.[30]

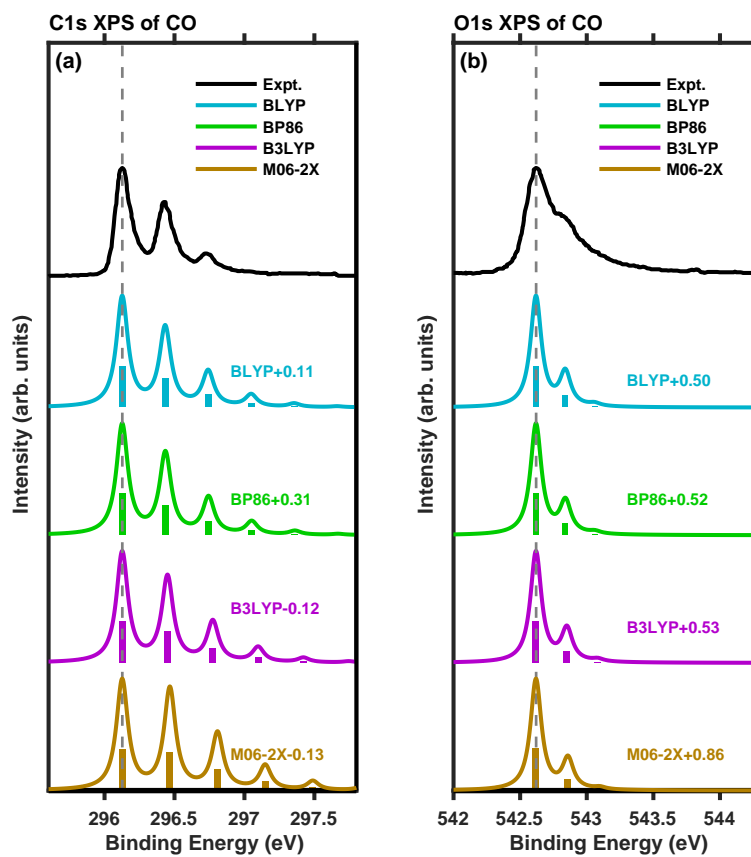


Figure 6: The same as Fig. 2 for simulated vibrationaly-resolved XPS spectra of CO: (a) C1s and (b) O1s edges. Experiment was taken from Hergenahn.[2]

References

- [1] Carravetta V, Couto R C and Ågren H 2022 *J. Phys.: Condens. Matter* **34** 363002
- [2] Hergenhahn U 2004 *J. Phys. B: At. Mol. Opt. Phys.* **37** R89–R135 and Fig. 5 therein, with the experimental C1s and O1s XPS spectra of CO, has been recaptured in our Fig. 6.
- [3] Svensson S 2005 *J. Phys. B: At. Mol. Opt. Phys.* **38** S821–S838
- [4] Siegbahn K 1969 *ESCA applied to free molecules* (North-Holland Publishing)
- [5] Gel’Mukhanov F, Mazalov L and Kondratenko A 1977 *Chem. Phys. Lett.* **46** 133–137
- [6] Chen C T, Ma Y and Sette F 1989 *Phys. Rev. A* **40** 6737–6740 ISSN 0556-2791 and Fig. 2(a) therein, with the experimental N1s XAS spectrum of N₂, has been recaptured in our Fig. 2(a).
- [7] Rennie E, Kempgens B, Köppe H, Hergenhahn U, Feldhaus J, Itchkawitz B, Kilcoyne A, Kivimäki A, Maier K, Piancastelli M and others 2000 *J. Chem. Phys.* **113** 7362–7375
- [8] Minkov I, Gel’Mukhanov F, Friedlein R, Osikowicz W, Suess C, Öhrwall G, Sorensen S L, Braun S, Murdey R, Salaneck W R and Ågren H 2004 *J. Chem. Phys.* **121** 5733–5739
- [9] Fronzoni G, Baseggio O, Stener M, Hua W, Tian G, Luo Y, Apicella B, Alfé M, de Simone M, Kivimäki A and Coreno M 2014 *J. Chem. Phys.* **141** 044313
- [10] Mosnier J P, Kennedy E T, van Kampen P, Cubaynes D, Guilbaud S, Sisourat N, Puglisi A, Carniato S and Bizau J M 2016 *Phys. Rev. A* **93** 061401
- [11] Vaz da Cruz V, Ertan E, Ignatova N, Couto R C, Polyutov S, Odelius M, Kimberg V and Gel’Mukhanov F 2018 *Phys. Rev. A* **98** 012507
- [12] Michelitsch G S and Reuter K 2019 *J. Chem. Phys.* **150** 074104
- [13] Kjellsson L 2021 *X-ray spectroscopy on diatomic and cationic molecules* Ph.D. thesis Uppsala University
- [14] Huang M, Li C and Evangelista F A 2022 *J. Chem. Theory Comput.* **18** 219–233 ISSN 1549-9618, 1549-9626
- [15] Schippers S, Hillenbrand P M, Perry-Sassmannshausen A, Buhr T, Fuchs S, Reinwardt S, Trinter F, Müller A and Martins M 2023 *ChemPhysChem* ISSN 1439-4235, 1439-7641

- [16] Besley N A 2020 *Acc. Chem. Res.* **53** 1306–1315 ISSN 0001-4842, 1520-4898
- [17] Duschinsky F 1937 *Acta Physicochim. URSS* **7**
- [18] Hua W, Tian G and Luo Y 2020 *Phys. Chem. Chem. Phys.* **22** 20014–20026 ISSN 1463-9076, 1463-9084
- [19] Wei M, Cheng X, Zhang L, Zhang J R, Wang S Y, Ge G, Tian G and Hua W 2022 *Phys. Rev. A* **106** 022811 ISSN 2469-9926, 2469-9934
- [20] Cheng X, Wei M, Tian G, Luo Y and Hua W 2022 *J. Phys. Chem. A* **126** 5582–5593 ISSN 1089-5639, 1520-5215
- [21] Couto R C, Hua W, Lindblad R, Kjellsson L, Sorensen S L, Kubin M, Bülow C, Timm M, Zamudio-Bayer V, Von Issendorff B, Söderström J, Lau J T, Rubensson J E, Ågren H and Carravetta V 2021 *Phys. Chem. Chem. Phys.* **23** 17166–17176 ISSN 1463-9076, 1463-9084
- [22] Prendergast D and Galli G 2006 *Phys. Rev. Lett.* **96** 215502 ISSN 0031-9007, 1079-7114
- [23] Minkov I, Gelmukhanov F, Ågren H, Friedlein R, Suess C and Salaneck W R 2005 *J. Phys. Chem. A* **109** 1330–1336
- [24] Triguero L, Pettersson L G M and Ågren H 1998 *Phys. Rev. B* **58** 8097–8110
- [25] Jolly W L and Hendrickson D N 1970 *J. Am. Chem. Soc.* **92** 1863–1871
- [26] Ehara M, Nakatsuji H, Matsumoto M, Hatamoto T, Liu X J, Lischke T, Prümper G, Tanaka T, Makochekanwa C, Hoshino M, Tanaka H, Harries J R, Tamenori Y and Ueda K 2006 *J. Chem. Phys.* **124** 124311 ISSN 0021-9606, 1089-7690
- [27] Püttner R, Dominguez I, Morgan T J, Cisneros C, Fink R F, Rotenberg E, Warwick T, Domke M, Kaindl G and Schlachter A S 1999 *Phys. Rev. A* **59** 3415–3423 ISSN 1050-2947, 1094-1622 and Fig. 1 therein, with the experimental O1s XAS spectrum of CO, has been recaptured in our Fig. 4(b)
- [28] Carniato S, Bizau J M, Cubaynes D, Kennedy E T, Guilbaud S, Sokell E, McLaughlin B and Mosnier J P 2020 *Atoms* **8** 67 ISSN 2218-2004
- [29] Lindblad R, Kjellsson L, Couto R, Timm M, Bülow C, Zamudio-Bayer V, Lundberg M, von Issendorff B, Lau J, Sorensen S, Carravetta V, Ågren H and Rubensson J E 2020 *Phys. Rev. Lett.* **124** 203001 ISSN 0031-9007, 1079-7114 and Fig. 2 therein, with the experimental N1s XAS spectra of N_2^+ , has been recaptured in our Fig. 2(b).

- [30] Couto R C, Kjellsson L, Ågren H, Carravetta V, Sorensen S L, Kubin M, Bülow C, Timm M, Zamudio-Bayer V, von Issendorff B, Lau J T, Söderström J, Rubensson J E and Lindblad R 2020 *Phys. Chem. Chem. Phys.* **22** 16215–16223 and Fig. 2(a) therein, with the experimental C1s and O1s XAS spectra of CO⁺, has been recaptured in our Fig. 5.
- [31] Lindblad R, Kjellsson L, De Santis E, Zamudio-Bayer V, von Issendorff B, Sorensen S L, Lau J T, Hua W, Carravetta V, Rubensson J E, Ågren H and Couto R C 2022 *Phys. Rev. A* **106** 042814 ISSN 2469-9926, 2469-9934 and Fig. 3 therein, with the experimental N1s and O1s XAS spectra of NO⁺, has been recaptured in our Fig. 3.
- [32] Rocha A B 2011 *J. Chem. Phys.* **134** 024107
- [33] Martins M, Reinwardt S, Schunck J O, Schwarz J, Baev K, Müller A, Buhr T, Perry-Sassmannshausen A, Klumpp S and Schippers S 2021 *J. Phys. Chem. Lett.* **12** 1390–1395
- [34] Cerezo J and Santoro F 2023 *J. Comput. Chem.* **44** 626–643 ISSN 0192-8651, 1096-987X
- [35] Wei M, Zhang L, Tian G and Hua W 2023 Vibronic fine structure in the nitrogen 1s photoelectron spectra from Franck-Condon simulations II: Indoles arXiv:2307.01510 [physics]
- [36] Gel'mukhanov F and Ågren H 1999 *Phys. Rep.* **312** 87–330 ISSN 03701573
- [37] Zhang L, Ge G, Wei M and Hua W Vibrationally-resolved x-ray spectra of diatomic systems. II. Time-dependent wavepacket simulations to be submitted
- [38] Sharp T and Rosenstock H 1964 *J. Chem. Phys.* **41** 3453–3463
- [39] Ruhoff P T 1994 *Chem. Phys.* **186** 355–374
- [40] Ruhoff P T and Ratner M A 2000 *Int. J. Quantum Chem.* **77** 383–392
- [41] Bagus P S 1965 *Phys. Rev.* **139**(3A) A619–A634
- [42] Triguero L, Plashkevych O, Pettersson L and Ågren H 1999 *J. Electron. Spectrosc. Relat. Phenom.* **104** 195–207 ISSN 03682048
- [43] Gordon M S and Schmidt M W 2005 Advances in electronic structure theory *Theory and Applications of Computational Chemistry* (Elsevier) pp 1167–1189 ISBN 978-0-444-51719-7
- [44] Schmidt M W, Baldrige K K, Boatz J A, Elbert S T, Gordon M S, Jensen J H, Koseki S, Matsunaga N, Nguyen K A, Su S, Windus T L, Dupuis M and Montgomery J A 1993 *J. Comput. Chem.* **14** 1347–1363 ISSN 0192-8651, 1096-987X

- [45] Becke A D 1988 *Phys. Rev. A* **38** 3098–3100 ISSN 0556-2791
- [46] Lee C, Yang W and Parr R G 1988 *Phys. Rev. B* **37** 785–789 ISSN 0163-1829
- [47] Perdew J P 1986 *Phys. Rev. B* **33** 8822–8824 ISSN 0163-1829
- [48] Becke A D 1993 *J. Chem. Phys.* **98** 5648–5652 ISSN 0021-9606, 1089-7690
- [49] Zhao Y and Truhlar D G 2008 *Theor. Chem. Acc.* **119** 525–525 ISSN 1432-881X, 1432-2234
- [50] Dunning T H 1989 *J. Chem. Phys.* **90** 1007–1023 ISSN 0021-9606, 1089-7690
- [51] Kendall R A, Dunning T H and Harrison R J 1992 *J. Chem. Phys.* **96** 6796–6806 ISSN 0021-9606, 1089-7690
- [52] Kutzelnigg W, Fleischer U and Schindler M 1990 The IGLO-Method: Ab-initio Calculation and Interpretation of NMR Chemical Shifts and Magnetic Susceptibilities *Deuterium and Shift Calculation* vol 23 ed Diehl P, Fluck E, Günther H, Kosfeld R and Seelig J (Berlin, Heidelberg: Springer Berlin Heidelberg) pp 165–262 ISBN 978-3-642-75934-5 978-3-642-75932-1 series Title: NMR Basic Principles and Progress
- [53] Sakai Y, Miyoshi E, Klobukowski M and Huzinaga S 1997 *J. Chem. Phys.* **106** 8084–8092
- [54] Noro T, Sekiya M and Koga T 1997 *Theor. Chem. Acc.* **98** 25–32
- [55] Segmented Gaussian Basis Set. <http://sapporo.center.ims.ac.jp/sapporo/>. Accessed on 2023-7-4.
- [56] See Supplemental Material at [URL will be inserted by publisher] for optimized Cartesian coordinates of all diatomic systems
- [57] Zschornack G H 2007 *Handbook of X-Ray Data* (New York: Springer)
- [58] Neeb M, Rubensson J E, Biermann M and Eberhardt W 1994 *J. Electron. Spectrosc. Relat. Phenom.* **67** 261–274 ISSN 03682048
- [59] Moitra T, Madsen D, Christiansen O and Coriani S 2020 *J. Chem. Phys.* **153** 234111 ISSN 0021-9606, 1089-7690
- [60] Hitchcock A and Brion C 1980 *J. Electron. Spectrosc. Relat. Phenom.* **18** 1–21 ISSN 03682048 and Fig. 5 therein, with the experimental N1s XAS spectrum of N₂, has been recaptured in our Fig. 2(a), and Fig. 6(a) therein, with the experimental C1s XAS spectrum of CO, has been recaptured in our Fig. 4(a).
- [61] Albritton D L, Schmeltkopf A L and Zare R N 1979 *J. Chem. Phys.* **71** 3271–3279 ISSN 0021-9606, 1089-7690

- [62] Laher R R and Gilmore F R 1991 *J. Phys. Chem. Ref. Data* **20** 685–712
ISSN 0047-2689, 1529-7845